Acta Pharmacologica Sinica

www.nature.com/aps

ARTICLE

C10ORF12 modulates PRC2 histone methyltransferase activity and H3K27me3 levels

Yi Shi[1], Hong-lei Ma[1], You-wen Zhuang[1,2], Xiao-xi Wang[1], Yi Jiang[1,2] and H. Eric Xu[1,2,3]

The polycomb repressive complex 2 (PRC2) catalyzes the methylation of histone H3 on lysine 27 (H3K27) to generate trimethyl-H3K27 (H3K27me3) marks, thereby leading to a repressive chromatin state that inhibits gene expression. C10ORF12 was recently identified as a novel PRC2 interactor. Here, we show that C10ORF12 specifically interacts with PRC2 through its middle region (positions 619–718). C10ORF12 significantly enhances the histone methyltransferase activity of PRC2 in vitro and dramatically increases the total H3K27me3 levels in HeLa cells. C10ORF12 also antagonizes Jarid2, which is an auxiliary factor of the PRC2.2 subcomplex, to promote increased H3K27me3 levels in HeLa cells. Moreover, C10ORF12 alters the substrate preference of PRC2. These results indicate that C10ORF12 functions as a positive regulator of PRC2 and facilitates PRC2-mediated H3K27me3 modification of chromatin. These findings provide new insight into the roles of C10ORF12 in regulating the activity of the PRC2 complex.

Keywords: PRC2; C10ORF12; H3K27me3; histone methyltransferase; epigenetic regulation; histone modification

Acta Pharmacologica Sinica (2019) 40:1457–1465; https://doi.org/10.1038/s41401-019-0247-3

INTRODUCTION

Epigenetic regulation in the form of histone modifications, the incorporation of histone variants, DNA methylation and demethylation, and noncoding RNAs has a critical role in modulating chromatin states and gene expression without altering DNA sequences [1–5]. In particular, polycomb repressive complexes 1 (PRC1) and 2 (PRC2) have been identified as crucial epigenetic regulators that form histone-modifying complexes and whose composition may be context-dependent within cells [2, 6–15]. PRC1 establishes repressive chromatin structures via the activity of the E3 ubiquitin ligase RING1A/B, which monoubiquitylates Lys119 of histone H2A [11, 12]. In addition, PRC2 represses the expression of genes involved in cell fate determination, cell differentiation, and cancer formation by mediating H3K27me3 modification of histones and other epigenetic mechanisms [5–8, 16–26]. Human PRC2 consists of three core members: enhancer of zeste homolog 2 (EZH2), embryonic ectoderm development (EED) factor, and suppressor of Zeste 12 (SUZ12) [7, 20–23]. Furthermore, several auxiliary subunits, including retinoblastoma suppressor-associated protein 46/48 (RbAp46/48), PCL, Jarid2, and AEBP2, have been identified that may regulate the HMTase activity of the PRC2 complex and its recruitment to chromatin [27–42]. The catalytic subunit of PRC2, EZH2, does not possess histone methyltransferase (HMTase) activity alone; rather, it requires coordination with at least two other PRC2 core components (EED and SUZ12) to acquire robust HMTase activity [43–45].

Subsequent investigations after the initial characterization of the PRC2 core complex suggested that PRC2 contains other auxiliary subunits and that its composition varies as a function of cellular contents during development [40]. The HMTase activity and recruitment of PRC2 to target genes are regulated by various auxiliary subunits such as PCL, Jarid2, AEBP2, and C17ORF96 that exhibit different biological functions in different cell types [46]. Mammalian PRC2 has recently been classified as comprising two distinct complexes, PRC2.1 and PRC2.2 [46, 47]. In addition to the core subunits of PRC2, PRC2.1 subcomplexes contain one of the three polycomb-like homologs (PHF1, MTF2, or PHF19) as well as either of two more recently discovered interactors, C17ORF96 (also termed EPOP) and C10ORF12. The relative abundances of the PRC2.1 subunits associated with the core PRC2 components change dramatically during the differentiation of mouse ESCs into neural progenitor cells. Specifically, MTF2 and C17ORF96 become less abundant, whereas PHF19 and C10ORF12 become more abundant [46, 48]. In contrast, PRC2.2 subcomplexes contain Jarid2 and AEBP2 and localize to the majority of PRC2 sites in stem cells [35]. Jarid2 and AEBP2 can directly bind to DNA and have been implicated in the recruitment of PRC2 and in the modulation of its enzymatic activity [46, 49].

C10ORF12 was recently discovered as a novel PRC2 interactor [48–52] that lacks apparent homologs in *Drosophila* but is otherwise conserved in organisms ranging from bony fishes to humans [50]. Overexpression of C10ORF12 results in strong repression of luciferase expression and significant trimethylation of H3K27 at the transcription start site of the luciferase gene, indicating that C10ORF12 may be a positive regulator of PRC2 HMTase activity [49]. C10ORF12 may recruit the PRC2–PCL complex to target genes [49] and stimulate the methyltransferase

[1]The CAS Key Laboratory of Receptor Research, VARI-SIMM Center, Center for Structure and Function of Drug Targets, Shanghai Institute of Materia Medica, Chinese Academy of Sciences, Shanghai 201203, China; [2]University of Chinese Academy of Sciences, Beijing 100049, China and [3]Laboratory of Structural Sciences, Van Andel Research Institute, Grand Rapids, MI 49503, USA
Correspondence: Yi Shi (shiyi@simm.ac.cn) or Yi Jiang (yijiang@simm.ac.cn) or H. Eric Xu (eric.xu@simm.ac.cn)

Received: 19 March 2019 Accepted: 5 May 2019
Published online: 11 June 2019

© CPS and SIMM 2019

activity of PRC2 in vitro and in vivo and is also essential for mouse development [53]. However, further investigation is required to elucidate the exact mechanism by which C10ORF12 influences the activity of the PRC2 complexes. Here, we investigated C10ORF12 −PRC2 interactions and proposed a possible mechanism by which C10ORF12 influences the biological function of PRC2.

MATERIALS AND METHODS

Construct design and molecular cloning

cDNAs for C10ORF12 (UniProtKB entry sequence A0PJI9) and the PRC2 subunits EZH2, EED, SUZ12, RbAp48, and AEBP2 (UniProtKB entry isoform sequences Q15910–1, O75530–1, Q15022, Q09028–1, and Q6ZN18–1, respectively) were synthesized by Genewiz. An engineered EZH2 construct (engEZH2 with the removal of residues 1–9, 183–210, and 351–425 and the replacement of residues 493–515 by a LGGGGSGGGGSGGGGSAAA linker) was designed using sequence alignments and previously reported structures [20, 21]. The C10ORF12 and PRC2 subunit cDNAs were cloned into the pFastBac HT A vector between the *Eco*RI and *Hin*dIII restriction sites for baculovirus expression. An expression cassette with a double His tag (HHHHHHSSGLVPRGSHMASHHHHHHHHHH, DHT), a GFP tag, and a TEV cleavage sequence was then introduced at the N terminus of C10ORF12 or Suz12 to facilitate the expression and purification of the target proteins. The inserted sequences of all clones were confirmed by DNA sequencing.

Expression of the PRC2 complex and C10ORF12 in sf9 cells

High titers of recombinant baculovirus carrying the PRC2 complex and C10ORF12 (> 10^9 viral particles/mL) were obtained using the Bac-to-Bac baculovirus expression system (Invitrogen, Carlsbad, CA, USA). The titer of each baculovirus stock was determined using the anti-baculovirus envelope gp64 antibody. To evaluate PRC2 expression, equal amounts of baculovirus for each subunit (DHT-GFP-Suz12 (1–693), engEZH2, EED(77–441), RbAp48FL, and AEBP2FL) were used to infect *Spodoptera frugiperda* (Sf9) cells at a density of 2.0×10^6 cells/mL and a multiplicity of infection (MOI) of five, followed by cultivation in ESF 921 medium. To determine C10ORF12 expression, baculovirus expressing C10ORF12 was used to infect sf9 cells at a density of 2.0×10^6 cells/mL and an MOI of five. Cells were harvested at 48 h post infection by centrifugation at 2000 r/min for 20 min. Cells were then stored at −80 °C until further use.

Affinity purification and size exclusion chromatography of the PRC2 complex and C10ORF12

Harvested cells were sonicated and subjected to centrifugation followed by collection of the supernatant. The solubilized PRC2 complex or C10ORF12 was purified by TALON affinity chromatography. Prior to loading, the TALON resin (Clontech Laboratories, Inc.) was equilibrated with five column volumes of binding buffer consisting of 20 mM Tris/HCl (pH 7.5) and 400 mM NaCl. Solubilized PRC2 complex or C10ORF12 was then loaded onto the column and bound for 2 h at 4 °C with continuous rotation. After binding, the TALON resin was eluted with three column volumes of the buffer described above supplemented with 200 mM imidazole and was then washed with 20 column volumes of binding buffer supplemented with 25 mM imidazole. The concentrations of the elution fractions containing purified PRC2 were determined using a Bradford assay and an appropriate standard curve. The fusion PRC2 or C10ORF12 protein was then cut using TEV protease at a ratio of 1:500 (w/w) with incubation overnight at 4 °C. Protein was concentrated to ~ 5 mg/mL and further purified with a Superdex 200 HiLoad 26/60 gel filtration column (GE Healthcare) equilibrated in SEC buffer (20 mM HEPES, pH 7.5; 200 mM NaCl). Protein fractions were identified at $OD_{280\ nm}$, and PRC2 fractions with the affinity tag removed were pooled and concentrated for subsequent analysis.

Size exclusion chromatography with multi-angle light scattering (SEC-MALS)

The average molecular mass of the C10ORF12-PRC2 complex was determined on a DAWN HELEOS-II instrument (Wyatt) connected in tandem to a high-performance liquid chromatography system (Agilent). A 10 μL sample with a protein concentration of 1 mg/mL was loaded on a Nanofilm SEC-500 (Sepax) column in size buffer (20 mM Tris-HCl, pH 8.0, 200 mM NaCl) with a flow rate set at 0.35 mL/min. The molecular weight of the complex was then calculated on the basis of the differential refractive index signal determined by the intensity of light scattering and the coinciding protein concentration [54].

Protein copurification pulldown assays

Protein copurification pulldown assays were performed following previously described protocols [55]. In brief, 40 mL of Sf9 cells was co-infected with baculovirus expressing StrepII-GFP-fusion C10ORF12 fragments and PRC2. Cells were then harvested after 48 h of infection and lysed using lysis buffer. Clarified lysates were loaded onto 20 μL of Strep-Tactin beads equilibrated with binding buffer containing 50 mM Tris, 150 mM NaCl and 0.05% Nonidet P-40 at pH 7.5 and were then washed with 20 column volumes of the binding buffer. The beads were collected by centrifugation and then analyzed using sodium dodecyl sulfate–polyacrylamide gel electrophoresis (SDS–PAGE). After electrophoresis, gels were stained with Coomassie blue for analysis.

HMTase activity assay

The HMTase activity of PRC2 was measured using Perkin Elmer AlphaLISA kits [56]. Enzymatic reactions were promoted by incubating 10 nM PRC2 with assay buffer (50 mM Tris-HCl, pH 8.0; 50 mM NaCl; 1 mM dithiothreitol; 0.01% Tween-20; and 0.01% bovine serum albumin) containing 100 nM biotinylated histone H3 (21–32) peptide substrate and 5 μM SAM for 120 min at room temperature. Anti-trimethyl-histone H3 lysine 27 (anti-H3K27me3) AlphaLISA Acceptor beads and Streptavidin Donor beads (0.08 mg/mL) were preincubated for 1 h in 1 × Epigenetics Buffer 1. The presence of the histone H3 product methyl marker was detected by the addition of the preincubated AlphaLISA beads (final concentration of 5 μg/mL). Activity was allowed to proceed for 1 h at room temperature. The assay plates were subsequently analyzed in a Perkin Elmer Envision plate reader using the AlphaLISA setting for optimal signal detection with a 615 nm filter after sample excitation at 680 nm. The emission signal at 615 nm was used to quantify HMTase activity. The activity of PRC2 in the absence of C10ORF12 was defined as the relative activity value of 1.0. The data are expressed as the means ± standard errors of the means (SEMs) of at least three independent experiments. Statistical analysis of the differences between PRC2 and PRC2 with C10ORF12FL or C10ORF12 (619–989) was conducted using GraphPad Prism 7.0. The significance of the differences was assessed using Student's *t* test ($P < 0.05$ was considered statistically significant).

H3K27 peptide and nucleosome binding assays

The H3K27 peptide and nucleosome binding assays were performed using AlphaScreen assays (Perkin Elmer) as previously described [57–59]. In brief, His tag proteins and biotinylated H3 (21–32)K27me0/1/2/3 peptides or biotinylated mononucleosomes (ABIN2669715, Active Motif) were mixed in 1 × assay buffer to a final concentration of 100 nM and incubated for 30 min at room temperature. A 1:1 mixture of nickel-chelating acceptor and streptavidin-conjugated donor beads was then added to a final concentration of 5 μg/mL, and the plates were incubated for an additional 30 min in the dark at room temperature. After incubation, the plates were analyzed using a PerkElmer Envision plate reader with the AlphaScreen setting for

optimal signal detection with a 615 nm filter after sample excitation at 680 nm. The emission signal at 615 nm was then used to quantify H3K27 peptide binding. The resulting data are expressed as the means ± SEMs of at least three independent experiments. Statistical analysis of the differences between PRC2 and PRC2 with C10ORF12FL or C10ORF12 (619–989) was conducted in GraphPad Prism 7.0. The statistical significance of the differences was assessed using Student's *t* test ($P < 0.05$ was considered statistically significant).

Measurement of the H3K27me3 levels in HeLa cells by immunoblotting

HeLa cells (ATCC CCL-2) were cultured in Eagle's minimum essential medium (EMEM) supplemented with 10% fetal bovine serum at 37 °C and then were seeded in a 24-well plate at a density of 5000 cells/well. After 24 h of cultivation, 1 μg of pcDNA6.0-C10ORF12FL, C10ORF12 (1–619), MTF2, or Jarid2 (or combinations of these) was transfected using Lipofectamine 2000 (Life Technologies, Invitrogen) according to the manufacturer's protocols. Empty pcDNA6.0 vector was transfected and used as a negative control. The cells were then harvested and lysed after cultivation for 24 h. Equivalent concentrations of cell lysates were resolved by SDS−PAGE, and the H3K27me3 levels and total histone H3 levels were measured by immunoblotting with an anti-H3K27me3 antibody (Abcam, ab6147) and an anti-histone H3 antibody (Abcam, ab18521), respectively. β-Actin was used as the reference for normalizing the protein loading levels. The H3K27me3 levels were quantified by densitometry and normalized, where the H3K27me3 intensity was normalized to the relative intensity value of the empty pcDNA6.0 vector, which was considered to be 1.0. The data are expressed as the means ± SEMs of at least three independent experiments. Statistical analysis of the data was performed using GraphPad Prism 7.0 (GraphPad Software). Statistical significance of differences was measured using Student's *t* tests ($P < 0.05$ was considered statistically significant), and the following notations are used to denote different levels of statistical significance: $^{*}P < 0.05$, $^{**}P < 0.01$, $^{***}P < 0.001$, and $^{****}P < 0.0001$.

RESULTS

C10ORF12 forms a stable complex with PRC2 in vitro

To determine whether C10ORF12 and PRC2 are associated in vitro, DHT-GFP-C10ORF12 was co-expressed with PRC2 in sf9 cells, followed by purification with affinity chromatography and size exclusion chromatography. A single peak was observed at a 10.3-mL elution volume, corresponding to a size of 400 kDa (Fig. 1a), which was consistent with the expected molecular weight of the DHT-GFP-C10ORF12-PRC2 complex (400 kDa). SDS–PAGE analysis further showed that the peak contained C10ORF12 and all five components of PRC2: engEZH2, EED(77–441), Suz12 (1–693), RbAp48FL, and AEBP2FL. The stoichiometric ratio of the components was 1:1:1:1:1:1. These results indicate that C10ORF12 forms a stable monomeric complex with PRC2, suggesting the presence of a strong interaction between C10ORF12 and PRC2. The purified C10ORF12−PRC2 complex was then subjected to multiangle light scattering (MALS) analysis on a system connected in tandem to a high-performance liquid chromatography system. This approach allows the measurement of the molecular weight of a given complex independent of its conformation [60]. The SEC elution profile combined with the light scattering data and differential refractive index signals indicated the presence of a single peak, suggesting that the C10ORF12-PRC2 complex is highly homogeneous (Fig. 1b). Moreover, a molecular mass of 400 kDa was determined by SEC-MALS (Fig. 1b), which coincided with our independent SEC analyses (Fig. 1a).

The middle region (619–718) of C10ORF12 is essential for its interaction with PRC2

The C-terminal region of C10ORF12 is highly conserved, in contrast to the N-terminal region (Fig. S1). The secondary structure prediction by PSIPRED [61] demonstrated that C10ORF12 has a structured C terminus and a coiled N terminus (Fig. S2). To evaluate the minimal C10ORF12 fragment that associates with PRC2, StrepII pulldown assays were used to investigate the interaction between PRC2 and a series of C10ORF12 fragments comprising residue positions 1–618, 619–989, 718–989, and 807–989. Both the C10ORF12 full-length peptide, and the peptide fragment 619–989 bound PRC2, whereas the remaining peptide fragments (1–618, 718–989, and 807–989) did not bind PRC2

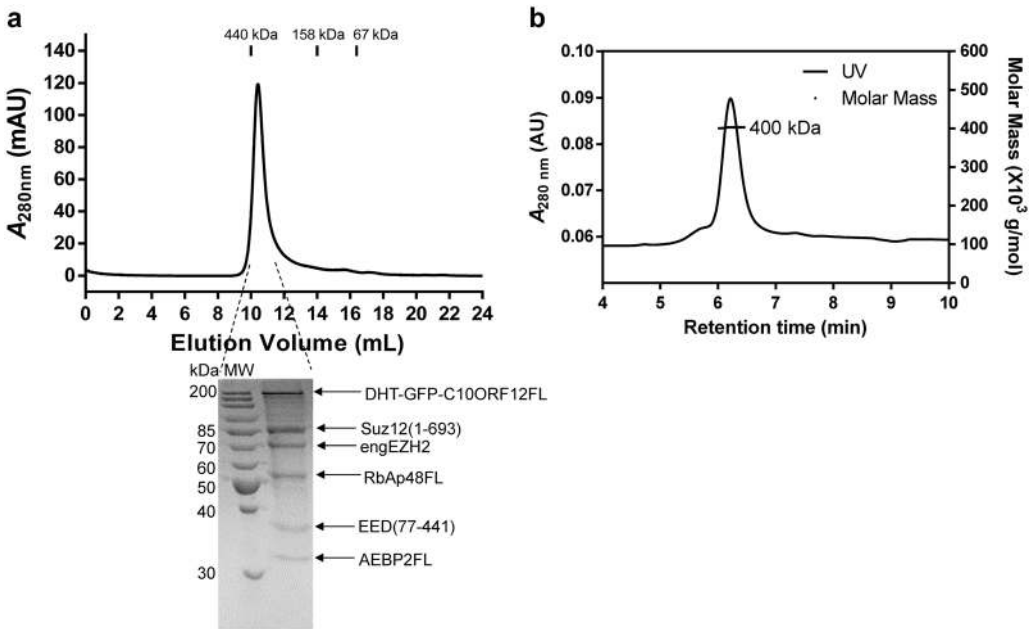

Fig. 1 C10ORF12 forms a stable complex with PRC2 in vitro. **a** Analysis of the C10ORF12−PRC2 complex using a Superdex 200 h 16/30 column (GE Health) with the fractions further analyzed by 12% SDS−PAGE and Coomassie blue staining. **b** SEC-MALS analysis of the C10ORF12-PRC2 complex

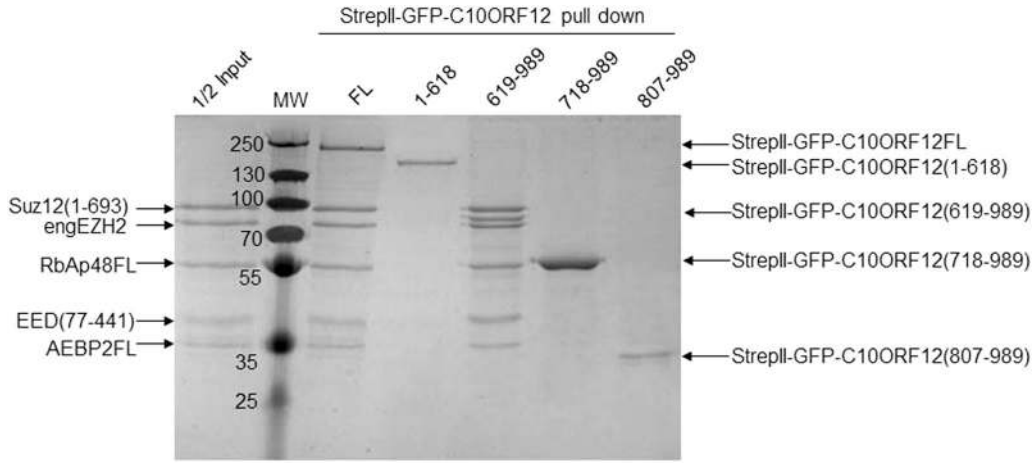

Fig. 2 The C-terminal region of C10ORF12 is essential for interaction with PRC2. The gel shows the results of SDS−PAGE analysis of C10ORF12 fragment pulldown assays as described below. Sf9 cells were co-infected with baculovirus expressing StrepII-GFP-fusion C10ORF12 fragments and PRC2. Cells were harvested after 48 h of infection and lysed using lysis buffer. Clarified lysates were then loaded onto 20 μL of Strep-Tactin beads equilibrated with binding buffer consisting of 50 mM Tris, pH 7.5; 150 mM NaCl; and 0.05% Nonidet P-40. The beads were then washed with 20 column volumes of the binding buffer. The beads were collected by centrifugation and analyzed with SDS–PAGE and gel staining with Coomassie blue

(Fig. 2). Thus, residues 619–718 of C10ORF12 are essential for PRC2 interaction, whereas the peptide region comprising residues 1–618 is not involved in PRC2 interaction.

C10ORF12 promotes the HMTase activity of PRC2 in vitro through its C-terminal region

The interaction between C10ORF12 and PRC2 suggested that C10ORF12 may affect PRC2 HMTase activity. Consequently, the enhancement of PRC2 methyltransferase activity by C10ORF12 was investigated. C10ORF12 and PRC2 were independently purified from Sf9 cells. Then, H3 (21–32)K27me0 peptides were used as PRC2 substrates, and increasing amounts of recombinant C10ORF12 were added. The abundance of the methylation product H3 (21–32)K27me3, which indicates the HMTase activity of PRC2, was measured using anti-H3K27me3 AlphaScreen beads. The H3K27me3 levels increased owing to the presence of C10ORF12 in a dose-dependent manner (Fig. 3). Specifically, the H3K27me3 levels were two-fold higher in the presence of 1 μM C10ORF12FL than without C10ORF12FL ($P < 0.01$) and fourfold higher in the presence of 6 μM C10ORF12FL ($P < 0.0001$). Similar results were obtained for C10ORF12 (619–989), further indicating that C10ORF12 can stimulate the HMTase activity of PRC2 via its C-terminal region comprising residues 619–989.

C10ORF12 enhances the total H3K27me3 levels in HeLa cells

To investigate the effect of C10ORF12 on the H3K27me3 levels in HeLa cells, we transfected C10ORF12 into HeLa cells and used anti-H3K27me3 antibodies to measure changes in the H3K27me3 levels (Fig. 4). Overexpression of C10ORF12FL enhanced the H3K27me3 levels in HeLa cells by 14-fold ($P < 0.0001$), whereas expression of C10ORF12 (619–989) enhanced the H3K27me3 levels in HeLa cells by eightfold ($P < 0.001$). In contrast, overexpression of C10ORF12 (1–618) did not affect the H3K27me3 levels. These results indicate that C10ORF12 can increase the total H3K27me3 levels in HeLa cells primarily via activity mediated by its C-terminal region.

C10ORF12 antagonizes Jarid2 to increase the H3K27me3 levels in HeLa cells

The PRC2 auxiliary factor Jarid2 has been reported to modulate the HTMase activity of PRC2 and its recruitment to chromatin [31, 38–40, 62–65]. Consequently, we evaluated whether C10ORF12 coordinates with Jarid2 to increase the H3K27me3

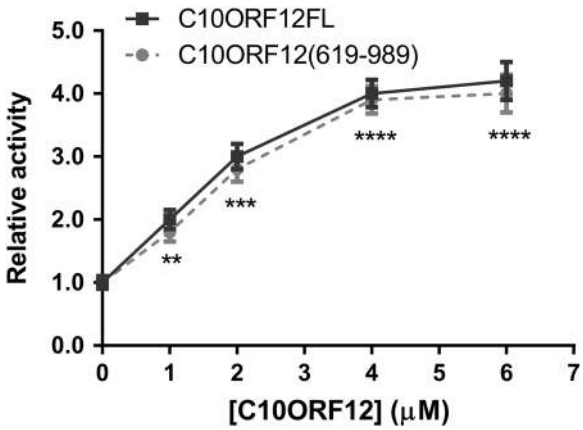

Fig. 3 C10ORF12 promotes the HMTase activity of PRC2 in vitro. The plot shows the relative HMTase activity of PRC2 in the presence of increasing concentrations of C10ORF12. PRC2 HMTase assays were performed using Perkin Elmer AlphaLISA kits. The PRC2 complex at a concentration of 10 nM was added to HMT Buffer (50 mM Tris-HCl, pH 8.0; 50 mM NaCl; 1 mM DTT; 0.01% Tween-20; and 0.01% BSA) supplemented with increasing concentrations (0–4 μM) of C10ORF12, 100 nM biotinylated H3 (21–32)K27me0 peptide, and 5 μM SAM. After incubating for 2 h at room temperature, 5 μg/mL anti-H3K27me3 beads and 5 μg/mL streptavidin beads were added, and the mixture was again incubated for 1 h at room temperature. The activity was then analyzed using a Perkin Elmer Envision plate reader. The activity of PRC2 in the absence of C10ORF12 was defined as a relative activity value of 1.0. The data are expressed as the means ± standard errors of the means (SEMs) of at least three independent experiments. Statistical analyses of the differences between PRC2 alone and PRC2 with C10ORF12FL or C10ORF12 (619–989) were analyzed using GraphPad Prism 7.0. The significance of the differences was assessed using Student's *t* test ($P < 0.05$ was considered statistically significant), and the following notations denote different levels of statistical significance: *$P < 0.05$, **$P < 0.01$, ***$P < 0.001$, and ****$P < 0.0001$

levels in HeLa cells. Individual overexpression of C10ORF12FL and Jarid2 enhanced the H3K27me3 levels in HeLa cells by 14-fold ($P < 0.0001$) and 5.3-fold ($P < 0.0001$), respectively. However, the stimulatory effect decreased to 2.7-fold when C10ORF12 and Jarid2 were overexpressed together, indicating that C10ORF12

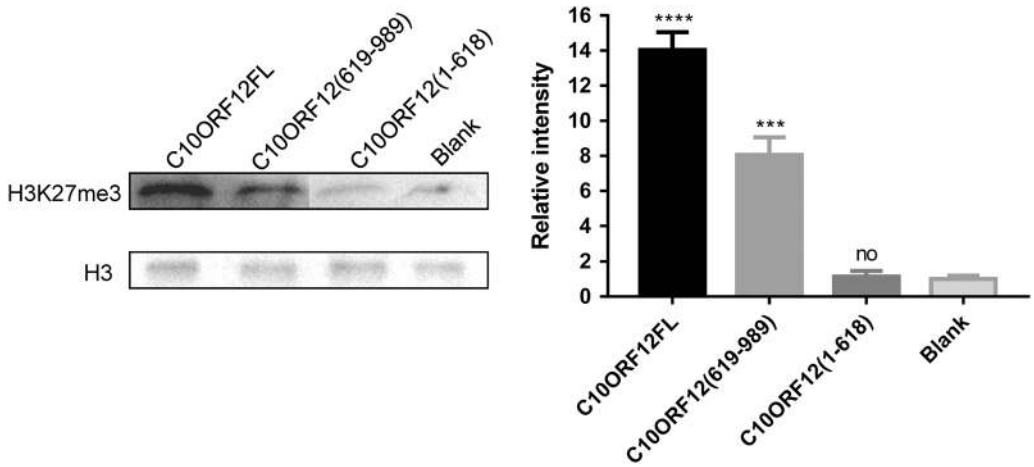

Fig. 4 C10ORF12 enhances the total H3K27me3 levels in HeLa cells. The H3K27me3 levels in HeLa cells that overexpressed various C10ORF12 fragments were detected using immunoblotting with anti-H3K27me3 antibodies. H3 levels measured by immunoblotting using anti-H3K27me3 antibodies were used as the internal reference. The H3K27me3 levels were quantified by densitometry and normalized to the H3 levels. The data are expressed as the means ± standard errors of the means (SEMs) of at least three independent experiments. Statistical differences between the C10ORF12 fragment overexpression vector and the blank empty vector control were analyzed in GraphPad Prism 7.0. The significance of the differences was assessed using Student's *t* test ($P < 0.05$ was considered statistically significant), and the following notations denote different levels of statistical significance: $^{*}P < 0.05$, $^{**}P < 0.01$, $^{***}P < 0.001$, and $^{****}P < 0.0001$

and Jarid2 antagonized each other's effect on the H3K27me3 levels in HeLa cells. C10ORF12 has been reported to be an auxiliary factor of the PRC2.1 subcomplex [48, 50, 53], whereas Jarid2 is a component of the PRC2.2 subcomplex [39, 40]. Our results indicate that independently, these factors stimulate PRC2 HMTase activity but compete with and antagonize each other when they interact with PRC2 simultaneously.

C10ORF12 alters the substrate preference of PRC2

To explore the mechanism by which C10ORF12 regulates PRC2 HMTase activity, we investigated the effect of C10ORF12 on the affinity of PRC2 for H3K27me0/1/2/3 peptides using AlphaScreen techniques. PRC2 bound each of the H3K27me0/1/2/3 peptides, whereas C10ORF12FL dramatically decreased the affinity of PRC2 for the H3K27me0 peptide (a 57% decrease with 1 μM C10ORF12FL, $P < 0.001$; a 73% decrease with 2 μM C10ORF12FL, $P < 0.001$), slightly decreased the affinity for the H3K27me1 peptide (an 8% decrease with 1 μM C10ORF12FL, $P > 0.05$; a 21% decrease with 2 μM C10ORF12FL, $P < 0.01$), slightly increased the affinity for the H3K27me2 peptide (a 7.5% increase with 1 μM C10ORF12FL, $P > 0.05$; a 16.6% increase with 2 μM C10ORF12FL, $P < 0.01$) and significantly increased the affinity for the H3K27me3 peptide (a 53% increase with 1 μM C10ORF12FL, $P < 0.01$; a 101% increase with 2 μM C10ORF12FL, $P < 0.001$) (Fig. 6). Similar results were observed for C10ORF12 (619–989) (Fig. 6). These results suggest that C10ORF12 alters the substrate preference of PRC2 by enhancing its affinity for the H3K27me3 and H3K27me2 peptides but decreasing its affinity for the H3K27me0 and H3K27me1 peptides. Our results are mutually consistent with previous results, indicating that C10ORF12 stimulates the PRC2-mediated catalysis of H3K27me2 conversion to H3K27me3.

C10ORF12 decreases the access of PRC2 to unmodified nucleosomes

As C10ORF12 alters the affinity of PRC2 for H3K27 peptides, a mechanism whereby C10ORF12 modifies the access of PRC2 to the nucleosome was investigated. AlphaScreen binding assays indicated that C10ORF12FL greatly decreased the access of PRC2 to unmodified nucleosomes (a 48% decrease with 1 μM C10ORF12FL, $P < 0.0001$; a 71% decrease with 2 μM C10ORF12FL, $P < 0.0001$; Fig. 7). Furthermore, C10ORF12 (619–989) exhibited similar results (Fig. 7). These data are consistent with those showing that C10ORF12 decreases the affinity of PRC2 for the H3K27me0 peptide.

DISCUSSION

Here, we observed that C10ORF12 forms a stable complex with PRC2 core subunits (Fig. 1) and that it interacts with PRC2 through its C-terminal region (619–989) (Fig. 2). Specifically, C10ORF12-significantly enhanced the ability of PRC2 to catalyze the conversion of unmethylated H3K27 to trimethylated H3K27 through its C-terminal region (619–989) (Fig. 3) and enhanced the total H3K27me3 levels in HeLa cells mainly through its C-terminal region (619–989) (Fig. 4). These results are consistent with those of Conway [53]. However, the stimulatory effect of C100RF12 (619–989) on H3K27me3 was weaker than that of the full-length C10ORF12, indicating that these effects may require synergistic activity of the C- and N-terminal regions, although the N-terminal region alone did not affect the H3K27me3 levels (Fig. 4). In particular, the N-terminal region (1–618) of C10ORF12 was reported to interact with the H3K9 methyltransferase G9a [53]. G9a-induced H3K9 methylation may promote H3K27 methylation, which could explain why the full-length C10ORF12 can achieve greater stimulation of H3K27me3 than the C-terminal region (619–989) alone in HeLa cells. The interaction between the N- and C-terminal regions of C10ORF12 and the way in which G9a-induced H3K9 methylation affects C10ORF12-promoted H3K27 methylation are unclear and require further investigation.

The composition of PRC2 dynamically changes during cellular development and differentiation. In particular, different auxiliary components, such as Jarid2, PCLs, and C10ORF12, interact with the core components of PRC2 to regulate the recruitment and HMTase activity of PRC2 at different developmental stages [48, 49, 51, 52]. However, the exact relationships between C10ORF12 and the other PRC2 components, including Jarid2, PCLs, and AEBP2, require further clarification. Our results indicate that C10ORF12 antagonizes the effect of Jarid2 on the H3K27me3 levels in HeLa cells (Fig. 5), suggesting that C10ORF12 competes with Jarid2 to regulate the HMTase activity of PRC2. In addition, the crystal structure of a heterotetrameric complex, consisting of Suz12, Rbbp4, Jarid2, and AEBP2 fragments indicates that the

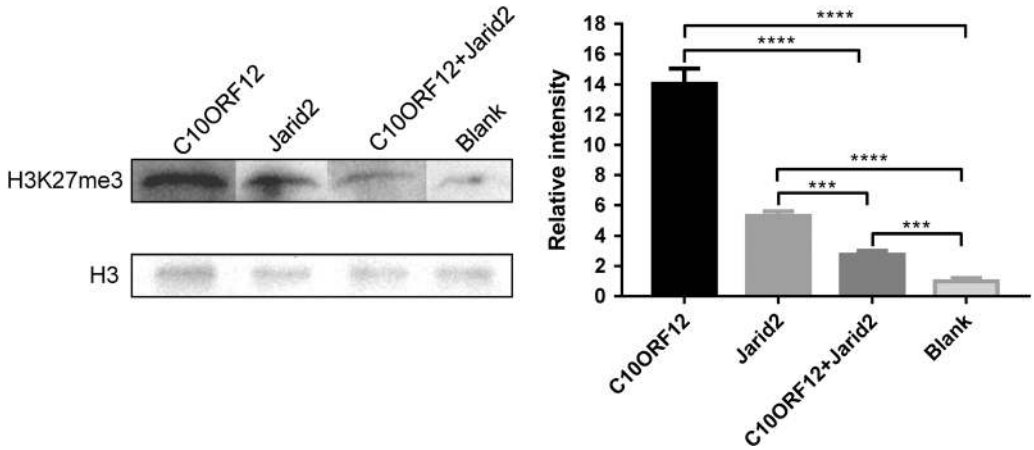

Fig. 5 C10ORF12 antagonizes the effects of Jarid2 on increasing the H3K27me3 levels in HeLa cells. The H3K27me3 levels were measured in HeLa cells overexpressing C10ORF12, Jarid2, and the combination of C10ORF12 and Jarid2 by immunoblotting with an anti-H3K27me3 antibody. H3 levels measured by immunoblotting with the anti-H3K27me3 antibody were used as the internal reference. The H3K27me3 levels were quantified by densitometry and were then normalized to the H3 levels. The data are expressed as the means ± standard errors of the means (SEMs) of at least three independent experiments. Statistical analyses were performed with GraphPad Prism 7.0. The significance of the differences was assessed using Student's *t* test ($P < 0.05$ was considered statistically significant), and the following notations denote different levels of statistical significance: *$P < 0.05$, **$P < 0.01$, ***$P < 0.001$, and ****$P < 0.0001$

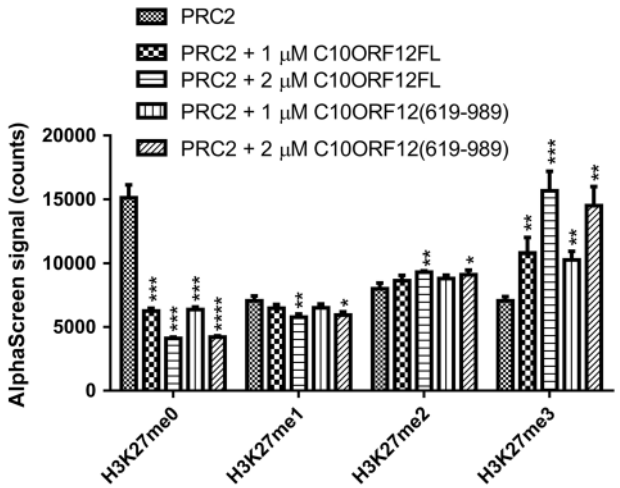

Fig. 6 C10ORF12 alters the substrate preference of PRC2. H3K27 peptide binding assays were performed using AlphaScreen kits (Perkin Elmer). His-tagged PRC2 complex at a concentration of 50 nM was added to AlphaScreen buffer containing increasing concentrations (0–2 μM) of C10ORF12, 100 nM biotinylated H3 (21–32)K27 peptide, 5 μg/mL nickel-chelating beads and 5 μg/mL streptavidin beads and incubated for 2 h at room temperature. The binding was then analyzed using a Perkin Elmer Envision plate reader. The data are expressed as the means ± standard errors of the means (SEMs) of at least three independent experiments. Statistical analysis of the differences between PRC2 alone and PRC2 with C10ORF12FL or C10ORF12 (619–989) was conducted in GraphPad Prism 7.0. The significance of the differences was assessed using Student's *t* test ($P < 0.05$ was considered statistically significant), and the following notations denote different levels of statistical significance. *$P < 0.05$, **$P < 0.01$, ***$P < 0.001$, and ****$P < 0.0001$

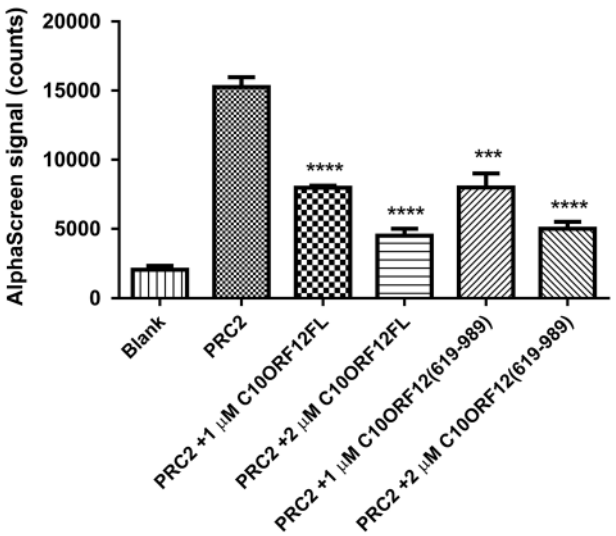

Fig. 7 C10ORF12 decreases the access of PRC2 to unmodified nucleosomes. Nucleosome binding was evaluated using AlphaScreen kits (Perkin Elmer). His-tagged PRC2 complex at a concentration of 50 nm was used with increasing amounts (0–2 μM) of C10ORF12, 50 nM biotinylated nucleosomes, 5 μg/mL nickel-chelating beads, and 5 μg/mL streptavidin beads. The mixtures were incubated in AlphaScreen buffer for 2 h at room temperature, and binding was then analyzed using a Perkin Elmer Envision plate reader. The data are expressed as the means ± standard errors of the means (SEMs) of at least three independent experiments. Statistical analysis of the differences between PRC2 alone and PRC2 with C10ORF12FL or C10ORF12 (619–989) were analyzed in GraphPad Prism 7.0. The significance of the differences was assessed using Student's *t* test ($P < 0.05$ was considered statistically significant), and the following notations denote different levels of statistical significance. *$P < 0.05$; **$P < 0.01$; ***$P < 0.001$; and ****$P < 0.0001$

PHF19 component of the PRC2.1 subcomplex competes with the PRC2.2 subcomplex component AEBP2 for binding to a non-canonical C2 domain of Suz12. Furthermore, the PRC2.2 subcomplex component Jarid2 and the C-terminal domain of the PRC2.1 subcomplex component C17ORF96/EPOP compete for binding to the ZnB-Zn motif of Suz12 [66]. Thus, both C10ORF12 and C17ORF96/EPOP compete with Jarid2. However, whether the mechanism underlying C10ORF12–Jarid2 competition is similar to that of C17ORF96/EPOP–Jarid2 competition is unclear and requires further investigation. Moreover, further clarification is needed as to whether C10ORF12 competes with AEBP2 or coordinates with PCLs.

Biochemical data and the crystal structures of the *Chaetomium thermophilum* and human PRC2 trimers indicate that the EZH2,

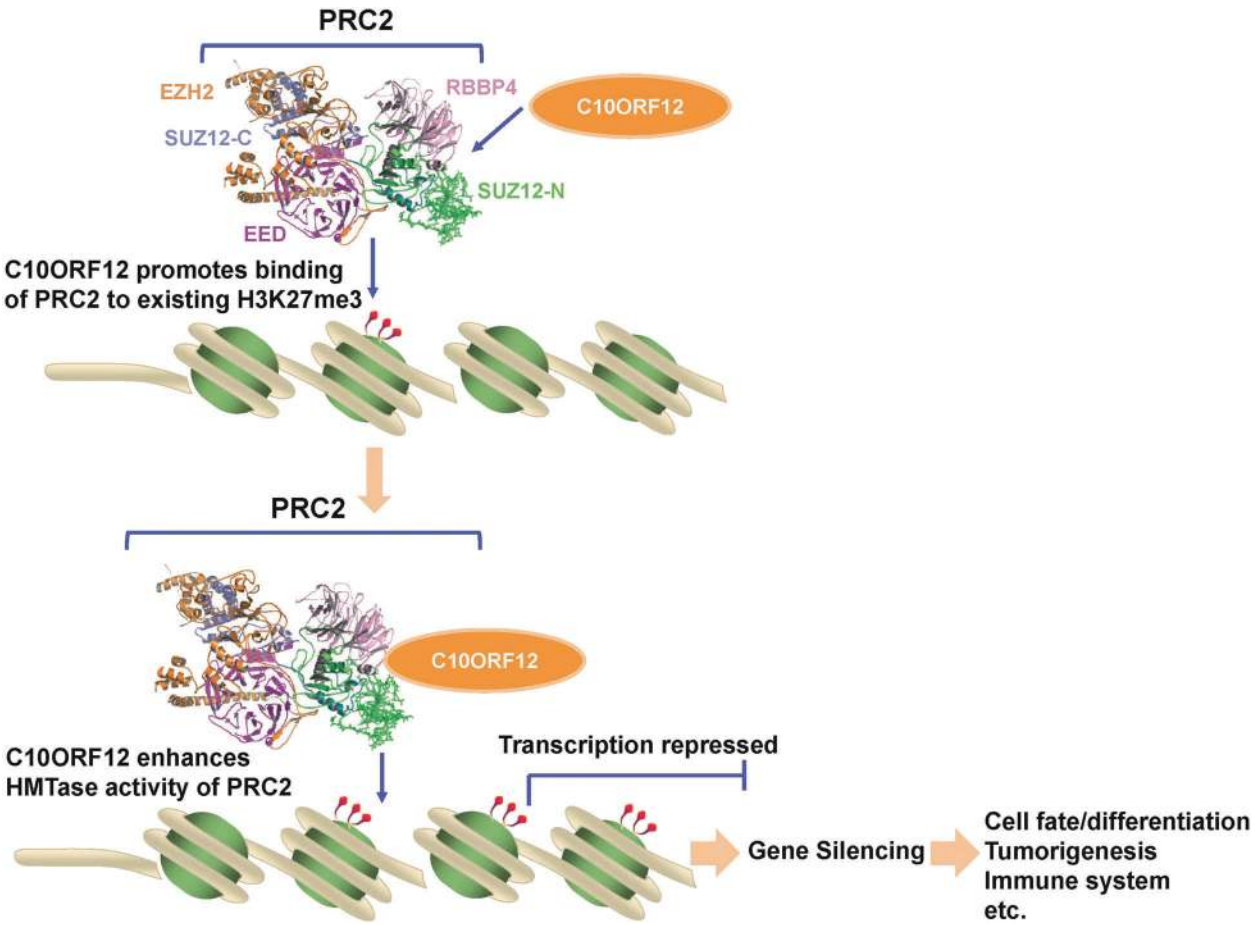

Fig. 8 A proposed model for the regulation of PRC2 by C10ORF12. The schematic shows a model wherein C10ORF12 helps to recruit PRC2 to established H3K27me3 and H3K27me2 sites. This recruitment then promotes the catalysis of H3K27me2 conversion to H3K27me3 and maintains the H3K27me3 state, thereby inducing targeted gene silencing that leads to cell fate decisions, cell differentiation, and cell cycle regulation, among other processes. The PRC2 complex structure was prepared with PyMOL using the cryo-EM structure deposited in PDB under accession number 6C23

EED, and VEFS domains of SUZ12 are bound to H3K27me3. Furthermore, other such analyses of the Jarid2K116me3 peptide have revealed that binding of H3K27me3 or Jarid2K116me3 to the EED and EZH2 SRM subdomains stabilizes the flexible EZH2 SET domain and thus enhances the HMTase activity of EZH2. [20–23, 67, 68]. These observations were confirmed and expanded upon by the recently published cryo-electron microscopy structure of PRC2 bound to a dinucleosome [69] and the Jarid2-PRC2 complex [70]. Our data show that C10ORF12 enhances binding to H3K27me3 peptides (Fig. 6) and decreases the affinity of PRC2 for H3K27me0 (Fig. 6) and unmodified nucleosomes (Fig. 7). C10ORF12 may also regulate PRC2 activity via a H3K27me3-mediated allosteric mechanism. However, additional biochemical and structural information for C10ORF12-PRC2 is needed to establish a model of regulation.

Based on these data, we propose a possible model for the regulation of PRC2 activity by C10ORF12. The model posits that C10ORF12 helps to recruit PRC2 to preexisting H3K27me3 sites to catalyze the conversion of H3K27 to H3K27me3 and maintain the H3K27me3 state. This process then induces transcriptional repression leading to cell fate decisions, cell differentiation, and cell cycle regulation, among other processes (Fig. 8). PRC2 and H3K27me3 have been reported to be involved in various cancers and are important drug targets in cancer therapy [71]. Indeed, several EZH2 inhibitors, such as EPZ6438 (tazemetostat), GSK-2816126, and CPI-1205, are undergoing clinical trials [16]. Consequently, C10ORF12 could represent a novel drug target in cancer therapy, owing to its role in PRC2 activity and H3K27me3 regulation. However, further investigation and validation of the role of C10ORF12 is needed.

In summary, our investigation of interactions between C10ORF12 and PRC2 revealed that C10ORF12 significantly enhances HMTase activity in vitro and in HeLa cells and alters the substrate preference of PRC2 via an interaction between its C-terminal region and PRC2. C10ORF12 antagonizes Jarid2, which is an auxiliary factor of the PRC2.2 subcomplex that promotes increased H3K27me3 levels in HeLa cells. A possible model for the regulation of PRC2 activity by C10ORF12 is proposed based on these results. These data and observations help form a better understanding of the roles and changes in PRC2 during cell development and differentiation.

ACKNOWLEDGEMENTS

This work was supported by the Strategic Priority Research Program of CAS (XDB08020303 to H.E.X.); the National Natural Science Foundation of China (31770796 to Y.J.); the Outstanding Young Scientist Foundation of CAS (to Y.J.); and the Youth Innovation Promotion Association of CAS (to Y.J.).

AUTHOR CONTRIBUTIONS

HEX, YS, and YJ designed the study. YS, HLM, YWZ, and XXW performed the experiments and analyzed the data. YS and YJ wrote the manuscript. HEX and YS.

revised the manuscript. All authors reviewed the results and approved the final version of the manuscript.

ADDITIONAL INFORMATION

The online version of this article (https://doi.org/10.1038/s41401-019-0247-3) contains supplementary material, which is available to authorized users.

Competing interests: The authors declare no competing interests.

REFERENCES

1. Arrowsmith CH, Bountra C, Fish PV, Lee K, Schapira M. Epigenetic protein families: a new frontier for drug discovery. Nat Rev Drug Discov. 2012;11:384–400.
2. Di Croce L, Helin K. Transcriptional regulation by Polycomb group proteins. Nat Struct Mol Biol. 2013;20:1147–55.
3. Copeland RA, Olhava EJ, Scott MP. Targeting epigenetic enzymes for drug discovery. Curr Opin Chem Biol. 2010;14:505–10.
4. Vermeulen M, Eberl HC, Matarese F, Marks H, Denissov S, Butter F, et al. Quantitative interaction proteomics and genome-wide profiling of epigenetic histone marks and their readers. Cell. 2010;142:967–80.
5. Margueron R, Reinberg D. Chromatin structure and the inheritance of epigenetic information. Nat Rev Genet. 2010;11:285–96.
6. Simon JA, Kingston RE. Occupying chromatin: polycomb mechanisms for getting to genomic targets, stopping transcriptional traffic, and staying put. Mol Cell. 2013;49:808–24.
7. Margueron R, Reinberg D. The Polycomb complex PRC2 and its mark in life. Nature. 2011;469:343–9.
8. Morey L, Helin K. Polycomb group protein-mediated repression of transcription. Trends Biochem Sci. 2010;35:323–32.
9. Zhen CY, Tatavosian R, Huynh TN, Duc HN, Das R, Kokotovic M, et al. Live-cell single-molecule tracking reveals co-recognition of H3K27me3 and DNA targets polycomb Cbx7-PRC1 to chromatin. Elife. 2016;5:pii: e17667.
10. Kahn TG, Dorafshan E, Schultheis D, Zare A, Stenberg P, Reim I, et al. Interdependence of PRC1 and PRC2 for recruitment to polycomb response elements. Nucleic Acids Res. 2016;44:10132–49.
11. McGinty RK, Henrici RC, Tan S. Crystal structure of the PRC1 ubiquitylation module bound to the nucleosome. Nature. 2014;514:591–6.
12. Blackledge NP, Farcas AM, Kondo T, King HW, McGouran JF, Hanssen LL, et al. Variant PRC1 complex-dependent H2A ubiquitylation drives PRC2 recruitment and polycomb domain formation. Cell. 2014;157:1445–59.
13. Yokobayashi S, Liang CY, Kohler H, Nestorov P, Liu Z, Vidal M, et al. PRC1 coordinates timing of sexual differentiation of female primordial germ cells. Nature. 2013;495:236–40.
14. Farcas AM, Blackledge NP, Sudbery I, Long HK, McGouran JF, Rose NR, et al. KDM2B links the polycomb repressive complex 1 (PRC1) to recognition of CpG islands. Elife. 2012;1:e00205.
15. Schuettengruber B, Bourbon HM, Di Croce L, Cavalli G. Genome regulation by polycomb and trithorax: 70 years and counting. Cell. 2017;171:34–57.
16. Shi Y, Wang XX, Zhuang YW, Jiang Y, Melcher K, Xu HE. Structure of the PRC2 complex and application to drug discovery. Acta Pharmacol Sin. 2017;38:963–76.
17. Yang YA, Yu J. EZH2, an epigenetic driver of prostate cancer. Protein Cell. 2013;4:331–41.
18. Conway E, Healy E, Bracken AP. PRC2 mediated H3K27 methylations in cellular identity and cancer. Curr Opin Cell Biol. 2015;37:42–8.
19. Melnick A. Epigenetic therapy leaps ahead with specific targeting of EZH2. Cancer Cell. 2012;22:569–70.
20. Justin N, Zhang Y, Tarricone C, Martin SR, Chen S, Underwood E, et al. Structural basis of oncogenic histone H3K27M inhibition of human polycomb repressive complex 2. Nat Commun. 2016;7:11316.
21. Broun A, Gajiwala KS, Deng YL, Liu W, Bolanos B, Bingham P, et al. Polycomb repressive complex 2 structure with inhibitor reveals a mechanism of activation and drug resistance. Nat Commun. 2016;7:11384.
22. Jiao L, Liu X. Structural basis of histone H3K27 trimethylation by an active polycomb repressive complex 2. Science. 2015;350:aac4383.
23. Ciferri C, Lander GC, Maiolica A, Herzog F, Aebersold R, Nogales E. Molecular architecture of human polycomb repressive complex 2. Elife. 2012;1:e00005.
24. Gaydos LJ, Wang W, Strome S. Gene repression. H3K27me and PRC2 transmit a memory of repression across generations and during development. Science. 2014;345:1515–8.
25. Shan Y, Liang Z, Xing Q, Zhang T, Wang B, Tian S, et al. PRC2 specifies ectoderm lineages and maintains pluripotency in primed but not naive ESCs. Nat Commun. 2017;8:672.
26. Huang X, Yan J, Zhang M, Wang Y, Chen Y, Fu X, et al. Targeting epigenetic crosstalk as a therapeutic strategy for EZH2-aberrant solid tumors. Cell. 2018;175:1–14.
27. Li H, Liefke R, Jiang J, Kurland JV, Tian W, Deng P, et al. Polycomb-like proteins link the PRC2 complex to CpG islands. Nature. 2017;549:287–91.
28. Choi J, Bachmann AL, Tauscher K, Benda C, Fierz B, Muller J. DNA binding by PHF1 prolongs PRC2 residence time on chromatin and thereby promotes H3K27 methylation. Nat Struct Mol Biol. 2017;24:1039–47.
29. Pasini D, Cloos PA, Walfridsson J, Olsson L, Bukowski JP, Johansen JV, et al. JARID2 regulates binding of the Polycomb repressive complex 2 to target genes in ES cells. Nature. 2010;464:306–10.
30. Shen X, Kim W, Fujiwara Y, Simon MD, Liu Y, Mysliwiec MR, et al. Jumonji modulates polycomb activity and self-renewal versus differentiation of stem cells. Cell. 2009;139:1303–14.
31. Peng JC, Valouev A, Swigut T, Zhang J, Zhao Y, Sidow A, et al. Jarid2/Jumonji coordinates control of PRC2 enzymatic activity and target gene occupancy in pluripotent cells. Cell. 2009;139:1290–302.
32. Brien GL, Gambero G, O'Connell DJ, Jerman E, Turner SA, Egan CM, et al. Polycomb PHF19 binds H3K36me3 and recruits PRC2 and demethylase NO66 to embryonic stem cell genes during differentiation. Nat Struct Mol Biol. 2012;19:1273–81.
33. Ballare C, Lange M, Lapinaite A, Martin GM, Morey L, Pascual G, et al. Phf19 links methylated Lys36 of histone H3 to regulation of Polycomb activity. Nat Struct Mol Biol. 2012;19:1257–65.
34. Schmitges FW, Prusty AB, Faty M, Stutzer A, Lingaraju GM, Aiwazian J, et al. Histone methylation by PRC2 is inhibited by active chromatin marks. Mol Cell. 2011;42:330–41.
35. Grijzenhout A, Godwin J, Koseki H, Gdula MR, Szumska D, McGouran JF, et al. Functional analysis of AEBP2, a PRC2 Polycomb protein, reveals a Trithorax phenotype in embryonic development and in ESCs. Development. 2016;143:2716–23.
36. Kim H, Kang K, Kim J. AEBP2 as a potential targeting protein for Polycomb Repression Complex PRC2. Nucleic Acids Res. 2009;37:2940–50.
37. Savla U, Benes J, Zhang J, Jones RS. Recruitment of Drosophila Polycomb-group proteins by Polycomblike, a component of a novel protein complex in larvae. Development. 2008;135:813–7.
38. Cooper S, Grijzenhout A, Underwood E, Ancelin K, Zhang T, Nesterova TB, et al. Jarid2 binds mono-ubiquitylated H2A lysine 119 to mediate crosstalk between Polycomb complexes PRC1 and PRC2. Nat Commun. 2016;7:13661.
39. Son J, Shen SS, Margueron R, Reinberg D. Nucleosome-binding activities within JARID2 and EZH1 regulate the function of PRC2 on chromatin. Genes Dev. 2013;27:2663–77.
40. Li G, Margueron R, Ku M, Chambon P, Bernstein BE, Reinberg D. Jarid2 and PRC2, partners in regulating gene expression. Genes Dev. 2010;24:368–80.
41. Landeira D, Sauer S, Poot R, Dvorkina M, Mazzarella L, Jorgensen HF, et al. Jarid2 is a PRC2 component in embryonic stem cells required for multi-lineage differentiation and recruitment of PRC1 and RNA Polymerase II to developmental regulators. Nat Cell Biol. 2010;12:618–24.
42. Wang X, Paucek RD, Gooding AR, Brown ZZ, Ge EJ, Muir TW, et al. Molecular analysis of PRC2 recruitment to DNA in chromatin and its inhibition by RNA. Nat Struct Mol Biol. 2017;24:1028–38.
43. Cao R, Zhang Y. SUZ12 is required for both the histone methyltransferase activity and the silencing function of the EED-EZH2 complex. Mol Cell. 2004;15:57–67.
44. Ketel CS, Andersen EF, Vargas ML, Suh J, Strome S, Simon JA. Subunit contributions to histone methyltransferase activities of fly and worm polycomb group complexes. Mol Cell Biol. 2005;25:6857–68.
45. Hansen KH, Bracken AP, Pasini D, Dietrich N, Gehani SS, Monrad A, et al. A model for transmission of the H3K27me3 epigenetic mark. Nat Cell Biol. 2008;10:1291–300.
46. Holoch D, Margueron R. Mechanisms regulating PRC2 recruitment and enzymatic activity. Trends Biochem. 2017;42:531–42.
47. Chittock EC, Latwiel S, Miller TC, Muller CW. Molecular architecture of polycomb repressive complexes. Biochem Soc Trans. 2017;45:193–205.
48. Kloet SL, Makowski MM, Baymaz HI, van Voorthuijsen L, Karemaker ID, Santanach A, et al. The dynamic interactome and genomic targets of Polycomb complexes during stem-cell differentiation. Nat Struct Mol Biol. 2016;23:682–90.
49. Hauri S, Comoglio F, Seimiya M, Gerstung M, Glatter T, Hansen K, et al. A high-density map for navigating the human polycomb complexome. Cell Rep. 2016;17:583–95.
50. Alekseyenko AA, Gorchakov AA, Kharchenko PV, Kuroda MI. Reciprocal interactions of human C10orf12 and C17orf96 with PRC2 revealed by BioTAP-XL cross-linking and affinity purification. Proc Natl Acad Sci USA. 2014;111:2488–93.
51. Smits AH, Jansen PW, Poser I, Hyman AA, Vermeulen M. Stoichiometry of chromatin-associated protein complexes revealed by label-free quantitative mass spectrometry-based proteomics. Nucleic Acids Res. 2013;41:e28.

52. Oliviero G, Brien GL, Waston A, Streubel G, Jerman E, Andrews D, et al. Dynamic protein interactions of the polycomb repressive complex 2 during differentiation of pluripotent cells. Mol Cell Proteom. 2016;15:3450–60.
53. Conway E, Jerman E, Healy E, Ito S, Holoch D, Oliviero G, et al. A family of vertebrate-specific polycombs encoded by the LCOR/LCORL genes balance PRC2 subtype activities. Mol Cell. 2018;70:408–21.e8.
54. Liu P, Jia MZ, Zhou XE, De Waal PW, Dickson BM, Liu B, et al. The structural basis of the dominant negative phenotype of the Galphai1beta1gamma2 G203A/A326S heterotrimer. Acta Pharm Sin. 2016;37:1259–72.
55. Hsu PL, Li H, Lau HT, Leonen C, Dhall A, Ong SE, et al. Crystal structure of the COMPASS H3K4 methyltransferase catalytic module. Cell. 2018;174:1106–16 e9.
56. Simard JR, Plant M, Emkey R, Yu V. Development and implementation of a high-throughput AlphaLISA assay for identifying inhibitors of EZH2 methyltransferase. Assay Drug Dev Technol. 2013;11:152–62.
57. Stuckey JI, Dickson BM, Cheng N, Liu Y, Norris JL, Cholensky SH, et al. A cellular chemical probe targeting the chromodomains of Polycomb repressive complex 1. Nat Chem Biol. 2016;12:180–7.
58. Qi W, Zhao K, Gu J, Huang Y, Wang Y, Zhang H, et al. An allosteric PRC2 inhibitor targeting the H3K27me3 binding pocket of EED. Nat Chem Biol. 2017;13:381–8.
59. Li L, Zhang H, Zhang M, Zhao M, Feng L, Luo X, et al. Discovery and molecular basis of a diverse set of polycomb repressive complex 2 inhibitors recognition by EED. PLoS One. 2017;12:e0169855.
60. Davidovich C, Goodrich KJ, Gooding AR, Cech TR. A dimeric state for PRC2. Nucleic Acids Res. 2014;42:9236–48.
61. McGuffin LJ, Bryson K, Jones DT. The PSIPRED protein structure prediction server. Bioinformatics. 2000;16:404–5.
62. Oksuz O, Narendra V, Lee CH, Descostes N, LeRoy G, Raviram R, et al. Capturing the onset of PRC2-mediated repressive domain formation. Mol Cell. 2018;70:1149–62 e5.
63. Sanulli S, Justin N, Teissandier A, Ancelin K, Portoso M, Caron M, et al. Jarid2 methylation via the PRC2 complex regulates H3K27me3 deposition during cell differentiation. Mol Cell. 2015;57:769–83.
64. Kalb R, Latwiel S, Baymaz HI, Jansen PW, Muller CW, Vermeulen M, et al. Histone H2A monoubiquitination promotes histone H3 methylation in Polycomb repression. Nat Struct Mol Biol. 2014;21:569–71.
65. Zhang Z, Jones A, Sun CW, Li C, Chang CW, Joo HY, et al. PRC2 complexes with JARID2, MTF2, and esPRC2p48 in ES cells to modulate ES cell pluripotency and somatic cell reprogramming. Stem Cells. 2011;29:229–40.
66. Chen S, Jiao L, Shubbar M, Yang X, Liu X. Unique structural platforms of Suz12 dictate distinct classes of PRC2 for chromatin binding. Mol Cell. 2018;69:840–52 e5.
67. Lee CH, Yu JR, Kumar S, Jin Y, LeRoy G, Bhanu N, et al. Allosteric activation dictates PRC2 activity independent of its recruitment to chromatin. Mol Cell. 2018;70:422–34.e6.
68. Lee CH, Holder M, Grau D, Saldaña-Meyer R, Yu JR, Ganai RA, et al. Distinct stimulatory mechanisms regulate the catalytic activity of polycomb repressive complex 2. Mol Cell. 2018;70:435–48.e5.
69. Poepsel S, Kasinath V, Nogales E. Cryo-EM structures of PRC2 simultaneously engaged with two functionally distinct nucleosomes. Nat Struct Mol Biol. 2018;25:154–62.
70. Kasinath V, Faini M, Poepsel S, Reif D, Feng XA, Stjepanovic G, et al. Structures of human PRC2 with its cofactors AEBP2 and JARID2. Science. 2018;359:940–4.
71. Kim KH, Roberts CW. Targeting EZH2 in cancer. Nat Med. 2016;22:128–34.